Preprints of the 10th IFAC International Symposium on Dynamics and Control of Process Systems
The International Federation of Automatic Control
December 18-20, 2013. Mumbai, India

Impact of delay on robust stable optimization of a CSTR with recycle stream ⋆

Darya Kastsian * **Martin Mönnigmann** *

* *Automatic Control and Systems Theory, Ruhr-Universität Bochum, 44801 Bochum, Germany (e-mails: darya.kastsian@rub.de, martin.moennigmann@rub.de).*

Abstract: We demonstrate that the normal vector method for robust optimization of nonlinear systems with uncertain parameters can be extended to systems with delays. A first-order exothermic irreversible reaction carried out in a CSTR with recycle stream serves as example for the broad class of nonlinear delay differential equations (DDE) with uncertain parameters. The stability boundaries that must be taken into account in the robust optimization consist of Hopf bifurcation points in this case. We show that (i) an unstable steady state of operation results if stability boundaries are neglected and (ii) a conservative optimal steady state results if the delay is ignored.

Keywords: Optimization, robust stability, steady-state stability, parametric uncertainty, time-delay, nonlinear programming, computer-aided system design, Hopf bifurcation

1. INTRODUCTION

Unconverted reactants are often separated from products and recycled back to the reactor in chemical plants. A combination of reaction and separation steps may be required, for example, to obtain the desired purity of a product stream. Several authors have studied stability properties of reactor-separator systems with recycle with numerical bifurcation techniques (see Engelborghs et al. (2002) and references on bifurcation theory of systems with delays therein). Pushpavanam and Kienle (2001) analyzed the stability of the steady states of a reactor-separator system, where a first-order exothermic irreversible reaction is carried out in a CSTR. Kiss et al. (2002) investigated the stability of CSTR-separator systems with recycle for polymerization reactions. In both studies, the impact of time delay associated with the recycle loop was neglected, however. A time delay naturally arises from a transportation lag between the units in the recycling process.

Balasubramanian et al. (2003) showed that it is important to take time delays into account when studying the stability of reactor-separator systems. The authors demonstrated that for some control strategies a time delay may cause instability of a first-order isothermal irreversible reaction in CSTR-separator systems with recycle. However, stability properties are independent of the delay if the fresh feed flow rate is flow controlled, the reactor holdup is constant, and the reactor is operated isothermally. For an exothermic first-order irreversible reaction in a nonisothermal CSTR, small delays even have a stabilizing effect (Balasubramanian et al., 2005; Gangadhar and Balasubramanian, 2010).

Matallana et al. (2011) optimized the capital cost of a CSTR-separator system operated under nonisothermal conditions. The authors seek the stable steady state with the largest domain of attraction. A two-level optimization approach involving nonsmooth functions was proposed. The economic objective is optimized in the first level. In the second level stability constraints are introduced and the domain of attraction is maximized. The effect of a time delay was neglected.

We consider a CSTR-separator system with delay. A first order exothermic irreversible reaction is carried out in the CSTR, which is operated nonisothermally. We optimize the production rate. We propose to use the so-called normal vector method, which ensures stability in a finite neighborhood around the optimal point, where the neighborhood can be chosen to account for uncertain model parameters (see. Sect. 4). The normal vector method was originally developed for the robust optimization of steady states of nonlinear ordinary differential equation systems (ODE) (Mönnigmann and Marquardt, 2002; Mönnigmann et al., 2007). It is the purpose of the present paper to demonstrate that the method can be applied to nonlinear DDE with uncertain parameters by applying it to the example outlined above.

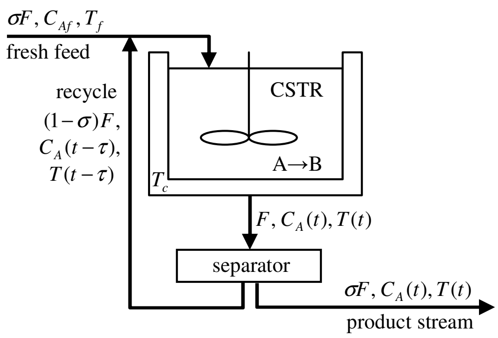

Fig. 1. Reactor-separator system with recycle.

⋆ Support by the Deutsche Forschungsgemeinschaft (DFG) under grant MO 1086/4 is gratefully acknowledged.

Table 1. Notation for parameters of model (1).

V	= reactor volume [m^3]
k_0	= kinetic constant [s^{-1}]
E	= activation energy of reaction [J mol^{-1}]
R	= ideal gas constant [J mol^{-1} K^{-1}]
ΔH	= heat of reaction [J mol^{-1}]
ρ	= molar density [mol m^{-3}]
C_p	= heat capacity [J mol^{-1} K^{-1}]
U	= heat transfer coefficient [W m^{-2} K^{-1}]
A	= heat transfer area [m^2]

2. REACTOR-SEPARATOR SYSTEM MODEL

We consider the simple reactor-separator process with recycle shown in Fig. 1. An exothermic first order reaction $A \rightarrow B$ takes place in the cooled CSTR. The effluent of the reactor is fed to a separator, where the unconverted reactant species A are separated from the product species B. The unconverted species A are mixed with the fresh feed and recycled back to the CSTR. We consider a process model that consists of the following material and energy balance equations (Lehman et al., 1994)

$$\begin{aligned}\frac{dC_A(t)}{dt} &= \frac{\sigma F}{V}C_{Af} - \frac{F}{V}C_A(t) + \frac{(1-\sigma)F}{V}C_A(t-\tau)\\ &\quad -k_0 e^{-\frac{E}{RT(t)}}C_A(t)\\ \frac{dT(t)}{dt} &= \frac{\sigma F}{V}T_f - \frac{F}{V}T(t) + \frac{(1-\sigma)F}{V}T(t-\tau)\\ &\quad +\frac{(-\Delta H)}{\rho C_p}k_0 e^{-\frac{E}{RT(t)}}C_A(t) - \frac{UA}{V\rho C_p}(T(t)-T_c),\end{aligned} \tag{1}$$

where C_A [mol m^{-3}] is the reactant concentration and T [K] is the reactor temperature. F [m^3 s^{-1}] denotes the total reactor flow rate. Note that the process model does not include the separator dynamics, but we merely assume that the desired separation ratio σ [-] can be obtained. The separation ratio attains values $\sigma \in [0, 1]$, where $\sigma = 0$ and $\sigma = 1$ correspond complete recycle and no recycle at all, respectively. The fresh feed to the reactor is provided with flow-rate σF [m^3 s^{-1}], concentration C_{Af} [mol m^{-3}], and temperature T_f [K]. The time delay associated with the recycle loop is denoted by τ [s]. The recycle stream is fed to the reactor with flow rate $(1-\sigma)F$ [m^3 s^{-1}], concentration $C_A(t-\tau)$ [mol m^{-3}], and temperature $T(t-\tau)$ [K]. A cooling jacket with the constant temperature T_c [K] is considered. The meaning of the remaining parameters of model (1) are explained in Tab. 1.

Following Lehman et al. (1994), we state the model (1) in dimensionless variables as

$$\begin{aligned}\frac{dx_1(t^*)}{dt^*} &= x_{10} - \frac{1}{\sigma}x_1(t^*) + (\frac{1}{\sigma}-1)x_1(t^*-\tau^*)\\ &\quad -Da\, e^{\frac{x_2(t^*)}{1+\frac{1}{\varepsilon}x_2(t^*)}}x_1(t^*)\\ \frac{dx_2(t^*)}{dt^*} &= x_{20} - \frac{1}{\sigma}x_2(t^*) + (\frac{1}{\sigma}-1)x_2(t^*-\tau^*)\\ &\quad +B\,Da\, e^{\frac{x_2(t^*)}{1+\frac{1}{\varepsilon}x_2(t^*)}}x_1(t^*) - \beta(x_2(t^*)-x_{2c}).\end{aligned} \tag{2}$$

The dimensional quantities of the model (2) are collected in Tab. 2. C_0 [mol m^{-3}] and T_0 [K] in Tab. 2 denote a reference concentration and temperature, respectively. The symbols t^* and τ^* denote the dimensionless time and delay. The dimensionless reactant concentration and dimensionless reactor temperature are denoted by x_1 and x_2, respectively. We assume that the following parameters are fixed in the model (2): $x_{10} = 1$, $x_{2c} = 0$, $\sigma = 0.25$, $\varepsilon = 12$, $\beta = 2.4$, $B = 20$, and $\tau^* = 0.4$. The dimensionless feed temperature x_{20} and Damköhler number Da are unknown uncertain parameters that will be subject to optimization.

Table 2. Dimensional quantities of model (2).

$t^* = \frac{\sigma F}{V}t$	$x_1 = \frac{C_A}{C_0}$	$x_{20} = \frac{T_f - T_0}{T_0}\varepsilon$	$Da = k_0\frac{V}{\sigma F}e^{-\varepsilon}$
$\tau^* = \frac{\sigma F}{V}\tau$	$x_{10} = \frac{C_{Af}}{C_0}$	$x_{2c} = \frac{T_c - T_0}{T_0}\varepsilon$	$B = \frac{(-\Delta H)C_0\varepsilon}{\rho C_p T_0}$
$\varepsilon = \frac{E}{RT_0}$	$x_2 = \frac{T - T_0}{T_0}\varepsilon$	$\beta = \frac{UA}{C_p\rho\sigma F}$	

The reactor-separator model (2) belongs to the class of DDE of the form

$$\frac{dx(t)}{dt} = f(x(t), x(t-\tau_1), \ldots, x(t-\tau_m), \alpha), \tag{3}$$

where $x(t) \in \mathbb{R}^{n_x}$, $\alpha \in \mathbb{R}^{n_\alpha}$, and $\tau_k \in \mathbb{R}^+$, $k = 1, \ldots, m$, denote state variables, uncertain parameters and delays, respectively. The function f maps from some open subset of $\mathbb{R}^{(m+1)n_x} \times \mathbb{R}^{n_\alpha}$ into $\mathbb{R}^{n_x}$ and is assumed to be sufficiently smooth. For the considered model (2) the number of variables, uncertain parameters, and delays in (3) are $n_x = 2$, $n_\alpha = 2$, and $m = 1$.

3. REFERENCE OPTIMIZATION WITHOUT STABILITY CONSTRAINTS

We would like to find an optimal and stable steady state of the reactor-separator model (2) that is robust with respect to parameter variations in a sense explained in detail further below. For reference, however, we first find a steady state solution of (2) without imposing any constraints on stability and robustness. The optimization problem that needs to be solved for this purpose has the form

$$\begin{aligned}\max_{x^{(0)},\alpha^{(0)}}\ & \phi(x^{(0)}, \alpha^{(0)})\\ \text{s.t. }\ & 0 = f(x^{(0)}, x^{(0)}, \ldots, x^{(0)}, \alpha^{(0)}) && \text{(4a)}\\ & 0 \le h(x^{(0)}, \alpha^{(0)}), && \text{(4b)}\end{aligned}$$

where $x^{(0)} \in \mathbb{R}^{n_x}$ and $\alpha^{(0)} \in \mathbb{R}^{n_\alpha}$ refer to the optimal steady state and the optimal point in the parameter space, respectively. The function $h : \mathbb{R}^{n_x} \times \mathbb{R}^{n_\alpha} \mapsto \mathbb{R}^{n_h}$, which defines feasibility constraints (4b), is assumed to be sufficiently smooth. The objective function $\phi : \mathbb{R}^{n_x \times n_\alpha} \mapsto \mathbb{R}$ models a profit that is to be maximized. The function ϕ is also assumed to be sufficiently smooth.

The state variables and parameters are $x = (x_1, x_2)^T$ and $\alpha = (Da, x_{20})^T$, respectively, for the reactor-separator system (2). We impose constraints of the type (4b) on the dimensionless feed temperature x_{20} and the dimensionless reactor temperature x_2. These constraints read $x_{20} \le 3$ and $x_2 \le 10$, respectively. We maximize the production rate of species B in the reactor-separator system. The production rate of B corresponds to the amount of converted species A and reads $\sigma F(C_{Af} - C_A)$. Since Da is proportional to $V/(\sigma F)$, the profit function to be maximized is chosen to be

$$\phi(x, \alpha) = c_\phi \frac{x_{10} - x_1}{Da}, \tag{5}$$

where a scaling factor c_ϕ is introduced to assign the value $\phi = 1$ to the solution of the reference optimization problem (4). The optimal solution of (4) reads

$$(Da^{(0)}, x_{20}^{(0)}) = (0.065, 3). \tag{6}$$

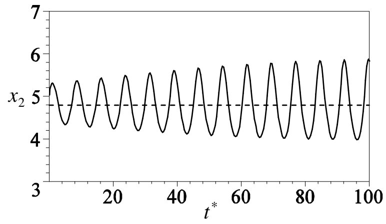

Fig. 2. Step response (solid) and steady state (dashed) for the parameters (6).

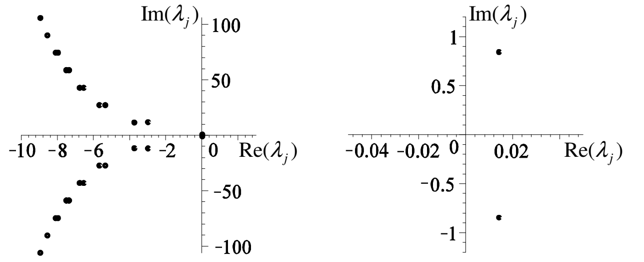

(a) (b)

Fig. 3. Characteristic roots λ_j (7) evaluated at optimal point (6). Part (b) is an enlargement of diagram (a).

The corresponding scaling factor c_ϕ is set to $c_\phi = \frac{1}{10.3}$. We obtained (6) and all other optimization results discussed below with the numerical optimization solver NPSOL (Gill et al., 2001).

Figure 2 shows a time series of (2) evaluated for the optimal parameters (6). The time series results after a step increase of the initial value $x_2(0)$ by 5%. Sustained oscillations arise and the solution converges to a limit cycle. The steady state that corresponds to (6) is unstable. This steady state is shown as a dashed line in Fig. 2.

3.1 Robust stability and feasibility

The stability properties of a steady state of the nonlinear DDE (3) are characterized by the real parts of the roots λ_j of the characteristic equation of the linearized DDE evaluated at that steady state. The characteristic equation reads

$$\det(\lambda I - J_0 - \sum_{k=1}^{m} J_k e^{-\lambda \tau_k}) = 0, \tag{7}$$

where $I \in \mathbb{R}^{n_x \times n_x}$ is the identity matrix, J_0 and J_k, $k = 1, \ldots, m$, are the Jacobian matrices with respect to variables $x(t)$ and $x(t - \tau_k)$, respectively. The Jacobians J_0 and J_k are evaluated at the steady state solution, i.e., $J_0 := J_0(x^{(0)}, \alpha^{(0)})$ and $J_k := J_k(x^{(0)}, \alpha^{(0)})$. The characteristic equation (7) has an infinite number of roots λ_j, $j \in \mathbb{N}$. If all λ_j satisfy $\mathrm{Re}(\lambda_j) < 0$ for the steady state of interest, then this steady state is a stable steady state of the system of nonlinear DDE (3) (Hale and Verduyn Lunel, 1993, Chap. 5).

Fig. 3 illustrates the rightmost characteristic roots of (7) for the reference optimization result (6) in the complex plane. The characteristic roots were obtained with DDE-BIFTOOL (Engelborghs et al., 2002). From Fig. 3b it is apparent that there exists a pair of complex characteristic roots with a positive real part. Continuation of steady states of (2) reveals that the reference optimal point

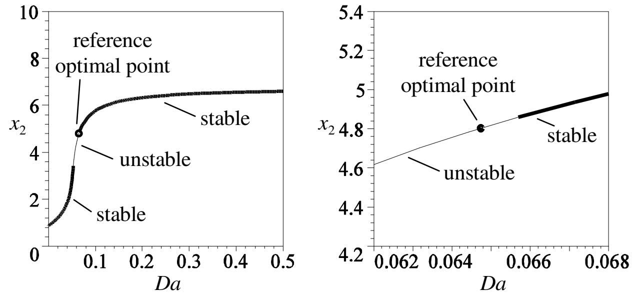

(a) (b)

Fig. 4. Continuation of steady states of (2) for $x_{20} = 3$. Solution (6) corresponds to the unstable steady state. Part (b) is an enlargement of diagram (a).

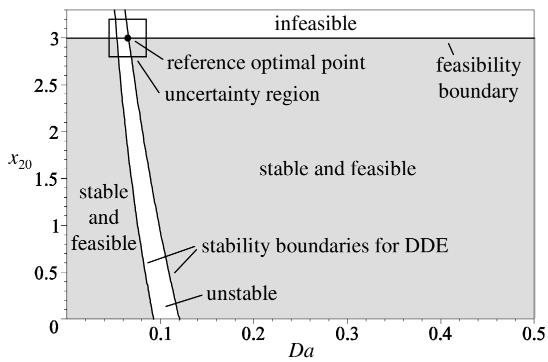

Fig. 5. Reference optimal point and regions with distinct dynamical properties of (2) in the space of uncertain parameters (Da, x_{20}).

is located on an unstable branch of steady states. The transitions from stable to unstable steady states in Fig. 4 correspond to Hopf bifurcations (see Engelborghs et al. (2002) and references therein for Hopf bifurcations of DDE).

We consider the dimensionless feed temperature x_{20} and the Damköhler number Da to be uncertain parameters in the sense that they cannot be fixed to precise values, but they may drift within certain error bars. Specifically, we assume

$$\begin{aligned}(Da, x_{20}) \in &[Da^{(0)} - \Delta Da, Da^{(0)} + \Delta Da] \times \\ &[x_{20}^{(0)} - \Delta x_{20}, x_{20}^{(0)} + \Delta x_{20}],\end{aligned} \tag{8}$$

where $\Delta Da = 0.02$ and $\Delta x_{20} = 0.2$ for the example treated here. Admittedly, (8) is a crude description of uncertain parameters. More precise descriptions, such as probability distributions, are rarely available in engineering applications, however.

3.2 Sketch of the main idea

Figure 5 shows the reference optimal point (6) in the space of the uncertain parameters (Da, x_{20}). The square centered at the optimal point marks the uncertainty region (8). The stability boundaries in Fig. 5 are obtained by continuation of the Hopf bifurcation points. We call a candidate steady state robust, if it is stable and feasible and if it remains stable and feasible as long as the parameters drift in the uncertainty region (8). We can enforce robust stability by guaranteeing the characteristic roots to remain in the open left half of the complex plane. This must be enforced for all steady states that can be attained in the neighborhood of the candidate steady state as the parameters are varied in the uncertainty region (8). Similarly, we can enforce robust feasibility by guaranteeing these steady states in the neighborhood of the candidate steady state to be feasible. These two robustness conditions are fulfilled if the robustness region marked by the square in Fig. 5 is located in the gray area. It is apparent from Fig. 5 that this is not the case for the reference point (6).

Note that the points at which a characteristic root moves from the left half into the right half of the complex plane are the bifurcation points of the dynamical system. Essentially, the normal vector constraints introduced in the following section restrict the optimization to the steady states that are robust by enforcing a back-off distance from bifurcation points and feasibility boundaries.

4. NORMAL VECTOR METHOD

The normal vector method is based on the geometric interpretation of stability and feasibility boundaries sketched in Sect. 3.2. Dobson (1993) proposed to characterize steady states by their distances to bifurcation boundaries measured along normal vectors in the parameter space. Mönnigmann and Marquardt (2002) showed that this characterization of the distance to stability and feasibility boundaries can be used to implement robustness constraints for the optimization of steady states of ODE systems. The approach has been extended to the robust optimization of fixed points of nonlinear discrete time systems (Kastsian and Mönnigmann, 2010), of periodically operated systems (Kastsian and Mönnigmann, 2012), and to the optimization of transient modes of operation of nonlinear continuous time systems (Gerhard et al., 2008).

We briefly summarize the idea of the normal vector constraints. As a preparation, we introduce a simple metric that measures each of the uncertain parameters α_i in units of its admissible uncertainty $\Delta\alpha_i$. This is equivalent to scaling the parameters according to $\alpha_i \to \alpha_i/\Delta\alpha_i$ and $\alpha_i^{(0)} \to \alpha_i^{(0)}/\Delta\alpha_i$. The hyperrectangular uncertain region (8) becomes a hypersquare under this scaling. It reads

$$\alpha_i \in [\alpha_i^{(0)} - 1, \alpha_i^{(0)} + 1] \quad \text{for } i = 1, \dots, n_\alpha. \tag{9}$$

The uncertainty region (9) can conveniently be overestimated by an n_α-dimensional hypersphere of radius $\sqrt{n_\alpha}$. Figure 6 shows a two-dimensional uncertainty region ($n_\alpha = 2$) and its overestimation by the circle of radius $\sqrt{2}$. We refer to the interior of the hypersphere as robustness region.

Consider a single stability or feasibility boundary of the type shown in Fig. 5. We sketch such a boundary along with a shaded region of parameter values that correspond to stable and feasible steady states in Fig. 6. We explained in Sect. 3.2 that any candidate optimal point $\alpha^{(0)}$ and its uncertainty region (9) has to lie in this shaded region. Figure 6 illustrates how to use the normal vector to the critical boundary to enforce this requirement. The normal vector constraints guarantee that the distance of $\alpha^{(0)}$ to the critical boundary is equal to, or larger than, the radius $\sqrt{n_\alpha}$ of the robustness region. Formally, the normal vector constraints read

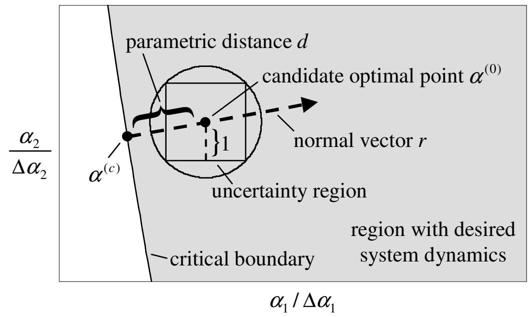

Fig. 6. A candidate optimal point $\alpha^{(0)}$ can be forced to lie in the region with desired system dynamics with the constraints on the parametric distance d.

$$\alpha^{(0)} = \alpha^{(c)} + d\frac{r}{\|r\|}, \qquad d \geq \sqrt{n_\alpha}, \tag{10}$$

where $r \in \mathbb{R}^{n_\alpha}$, $\alpha^{(c)}$ and $||\cdot||$ denote the normal vector, the closest point on the critical boundary and the Euclidean norm, respectively. If multiple critical boundaries exist, cf. Fig. 5, a normal vector constraint (10) must be stated for each critical boundary.

In order to implement the constraints (10), the normal vector r must be calculated as a function of the candidate optimal point $\alpha^{(0)}$. Mönnigmann and Marquardt (2002) presented a schema for deriving the normal vector systems (11) from the so-called augmented systems of the bifurcation points that are used in parameter continuation methods. This derivation is based on characterizing the normal space to the manifolds of bifurcation points in the space of the state variables x and uncertain parameters α, and on selecting the particular vector in this normal space that has no contribution in the state space. Since these steps are quite technical, we omit details here and report the resulting system for Hopf bifurcations of DDE in the appendix. In general the systems of equations for the calculation of normal vectors have the form

$$G^{(c)}(x^{(c)}, \bar{x}^{(c)}, \alpha^{(c)}, r) = 0, \tag{11}$$

where $(x^{(c)}, \alpha^{(c)})$ refers to a bifurcation point, $\bar{x}^{(c)}$ denotes a vector of auxiliary variables, and the superscript c is used to indicate the particular type of bifurcation point (Hopf throughout this paper). Similar systems of equations can be derived for normal vectors to feasibility boundaries. We refer to Mönnigmann and Marquardt (2002) for details. One feasibility and two stability boundaries due to Hopf bifurcations of DDE arise for the reactor-separator model with delay treated here.

It remains to augment the optimization problem (4) with the normal vector constraints (10). This results in the following optimization problem

$$\max_{x^{(0)},\alpha^{(0)}} \ \phi(x^{(0)}, \alpha^{(0)})$$

$$\text{s.t. } 0 = f(x^{(0)}, x^{(0)}, \dots, x^{(0)}, \alpha^{(0)}) \tag{12a}$$

$$0 \leq h(x^{(0)}, \alpha^{(0)}) \tag{12b}$$

$$0 = G^{(c,i)}(x^{(c,i)}, \bar{x}^{(c,i)}, \alpha^{(c,i)}, r^{(i)}), \forall i \in \mathcal{I} \tag{12c}$$

$$0 = \alpha^{(0)} - \alpha^{(c,i)} + d^{(i)}\frac{r^{(i)}}{\|r^{(i)}\|}, \forall i \in \mathcal{I} \tag{12d}$$

$$0 \leq d^{(i)} - \sqrt{n_\alpha}, \ \forall i \in \mathcal{I}. \tag{12e}$$

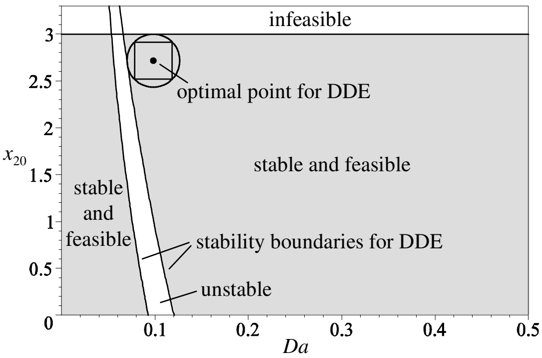

Fig. 7. Optimal point (13) obtained with the normal vector method for DDE.

Constraints (12a) and (12b) are the same as in (4). We assume that $i_{\max}$ critical boundaries exist. Equations (12c) describe these boundaries for all $i \in \mathcal{I} := \{1, ..., i_{\max}\}$. The corresponding normal vectors $r^{(i)}$ for all $i \in \mathcal{I}$ are stated in (12c). The constraints (12d) and (12e) enforce the parametric distances $d^{(i)}$ to each critical boundary. If solving (12) results in $d^{(i)} = \sqrt{n_\alpha}$, then the robustness region touches the ith critical boundary.

We stress that critical boundaries like those shown in Fig. 5 do not have to be precomputed before solving optimization problem (12). Their location can be detected automatically in the course of optimization. We refer to Mönnigmann et al. (2007) for details.

5. OPTIMIZATION OF THE REACTOR-SEPARATOR SYSTEM WITH STABILITY CONSTRAINTS

We apply the normal vector method to the optimization of the reactor-separator system (2). We consider the uncertainty region (8) and state the normal vector constraints (10) for the Hopf bifurcation boundaries and the feasibility boundary shown in Fig. 5, i.e., $i_{\max} = 3$ in (12). Maximizing the profit function ϕ (5) with the normal vector method results in the optimal point

$$(Da^{(0)}, x_{20}^{(0)}) = (0.098, 2.72). \tag{13}$$

This result corresponds to objective function value $\phi = 0.81$. Figure 7 shows the optimal point (13) in the parameter space. In contrast to the solution shown in Fig. 5, where constraints on stability were not considered, the optimal result obtained with the normal vector method is stable and feasible. Moreover, it is robust in the sense defined in Sect. 3.2, i.e. a stable and feasible steady state of model (2) exists for all parameter values in the robustness region (8). The real parts of all characteristic roots are negative for the optimal point (13). Figure 8a shows the rightmost characteristic roots for the optimal point. Figure 8b illustrates the location of the optimal point on the steady-state manifold in a one-parameter bifurcation diagram for the parameter $Da \in [0, 0.5]$. Note that this figure corresponds to a cut through Fig. 7. The step response shown in Fig. 4 corroborates that the optimal steady state is stable. The step response is obtained in the same manner as for Fig. 4, i.e. for an increase of value $x_2(0)$ by 5%.

Recall that for the optimal point (13) DDE (2) were considered with $\tau^* = 0.4$. To study the effect of the time delay we repeat the analysis and optimization of (2) for

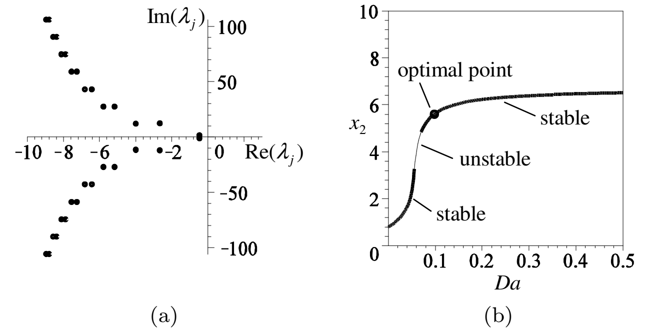

Fig. 8. Part (a) shows characteristic roots λ_j (7) evaluated at optimal point (13). Part (b) shows point (13) and continuation of steady states for $x_{20} = 2.72$.

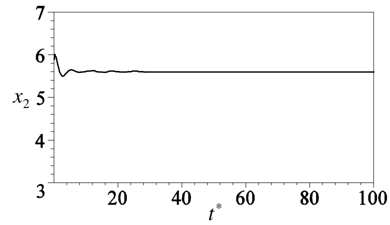

Fig. 9. Time series evaluated at optimal point (13).

$\tau^* = 0$. Figure 10 shows the stability boundaries of (2) for this case. These stability boundaries consist of Hopf bifurcation points of ODE. The stability boundaries for the DDE from Figs. 5 and 7 are also shown for comparison. It is apparent from Fig. 10 that there exists a region which contains steady states that are unstable if the time delay is neglected, but stable for $\tau^* = 0.4$.

We repeat the optimization (12) with normal vector constraints for the case $\tau^* = 0$. Note that this case corresponds to an optimization of an ODE system. The normal vector constraints for DDE given in the appendix also apply in the ODE case and they coincide with the normal vector constraints for the ODE published in Mönnigmann and Marquardt (2002). The optimization with the normal vector constraints for ODE results in

$$(Da^{(0)}, x_{20}^{(0)}) = (0.105, 2.72). \tag{14}$$

The objective function evaluates to $\phi = 0.77$ at this point, which is 4% lower than the value obtained for optimal

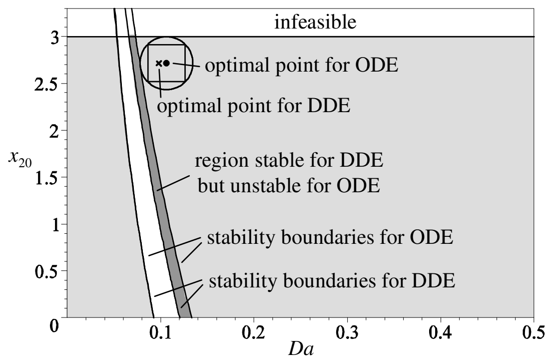

Fig. 10. Optimal point (14) obtained with the normal vector method for ODE ($\tau^* = 0$). Point (13) for DDE ($\tau^* = 0.4$) is shown for comparison.

point for DDE (13). Both Fig. 10 and the profit function values reveal that the delay has a small but a stabilizing effect for the example considered here.

6. CONCLUSIONS

We demonstrated that the normal vector method for robust optimization of uncertain systems of ordinary differential equations can be extended to the case of uncertain systems of delay differential equations (DDE). A simple reactor-separator system with delay in the recycle served as an example for the broad class of uncertain DDE. The optimal steady state of operation is unstable for this example. Therefore, a model-based optimization that does not take stability properties into account fails for this example. In contrast, a robust optimal point of operation can be found with the proposed method. We stress that the paper does not present a complete theory, but only demonstrates that the normal vector method can be extended to the case of uncertain DDE by example. In the particular example treated here, the delay turns out to have a stabilizing effect, which results in a higher profit function value for the system with delay than for the system without delay.

REFERENCES

Balasubramanian, P., Kosuri, M.R., Pushpavanam, S., and Kienle, A. (2003). Effect of delay on the stability of a coupled reactor-separator system. *Ind. Eng. Chem. Res.*, 42(16), 3758–3764.

Balasubramanian, P., Pushpavanam, S., Kienle, A., and Balaraman, K.S. (2005). Effect of delay on the stability of a coupled reactor-flash system sustaining an elementary non-isothermal reaction. *Ind. Eng. Chem. Res.*, 44(10), 3619–3625.

Dobson, I. (1993). Computing a closest bifurcation instability in multidimensional parameter space. *J. Nonlinear Sci.*, 3(3), 307–327.

Engelborghs, K., Luzyanina, T., and Roose, D. (2002). Numerical bifurcation analysis of delay differential equations using DDE-BIFTOOL. *ACM Trans. Math. Softw.*, 28(1), 1–21.

Gangadhar, N.R. and Balasubramanian, P. (2010). Numerical bifurcation analysis of delayed recycle stream in a continuously stirred tank reactor. In *AIP Conf. Proc. of the 2010 Int. Conf. Modeling, Optimization, and Computing*, 192–197.

Gerhard, J., Marquardt, W., and Mönnigmann, M. (2008). Normal vectors on critical manifolds for robust design of transient processes in the presence of fast disturbances. *SIAM J. Appl. Dyn. Syst.*, 7(2), 461–490.

Gill, P.E., Murray, W., Saunders, M.A., and Wright, M.H. (2001). *User's guide for NPSOL 5.0: A Fortran package for nonlinear programming.* Systems Optimization Laboratory, Stanford University, Stanford, USA. Tech. Rep. SOL 86-2.

Hale, J.K. and Verduyn Lunel, S.M. (1993). *Introduction to Functional Differential Equations.* Springer, New York.

Kastsian, D. and Mönnigmann, M. (2010). Robust optimization of fixed points of nonlinear discrete time systems with uncertain parameters. *SIAM J. Appl. Dyn. Syst.*, 9(2), 357–390.

Kastsian, D. and Mönnigmann, M. (2012). Robust optimization of periodically operated reactors with stability constraints. In *Proc. 2012 IEEE Int. Conf. Control Applications*, 184–189.

Kiss, A.A., Bildea, C.S., Dimian, A.C., and Iedema, P.D. (2002). State multiplicity in CSTR-separator-recycle polymerisation systems. *Chem. Eng. Sci.*, 57(4), 535–546.

Lehman, B., Bentsman, J., Lunel, S., and Verriest, E. (1994). Vibrational control of nonlinear time-lag systems with bounded delay: Averaging theory, stabilizability, and transient-behavior. *IEEE Trans. Autom. Control*, 39(5), 898–912.

Matallana, L.G., Blanco, A.M., and Bandoni, A.J. (2011). Design of reactor-separator-recycle systems based on the optimization of estimations of the domain of attraction. *Ind. Eng. Chem. Res.*, 50(11), 6769–6776.

Mönnigmann, M. and Marquardt, W. (2002). Normal vectors on manifolds of critical points for parametric robustness of equilibrium solutions of ODE systems. *J. Nonlinear Sci.*, 12(2), 85–112.

Mönnigmann, M., Marquardt, W., Bischof, C.H., Beelitz, T., Lang, B., and Willems, P. (2007). A hybrid approach for efficient robust design of dynamic systems. *SIAM Rev.*, 49(2), 236–254.

Pushpavanam, S. and Kienle, A. (2001). Nonlinear behavior of an ideal reactor separator network with mass recycle. *Chem. Eng. Sci.*, 56(8), 2837–2849.

Appendix A. NORMAL VECTOR SYSTEM FOR HOPF BIFURCATIONS OF DDE

The normal vector system (11) for Hopf bifurcation of DDE is denoted by

$$G^{(\mathrm{Hopf})}(x^{(\mathrm{Hopf})}, \bar{x}^{(\mathrm{Hopf})}, \alpha^{(\mathrm{Hopf})}, r) = 0.$$

It reads as the following system of $6n_x + n_\alpha + 4$ equations

$$
\begin{aligned}
f &= 0\\
J_0 w^{(1)} + \sum_{k=1}^{m} \left(J_k w^{(1)} c_k + J_k w^{(2)} s_k \right) + \omega w^{(2)} &= 0\\
J_0 w^{(2)} + \sum_{k=1}^{m} \left(J_k w^{(2)} c_k - J_k w^{(1)} s_k \right) - \omega w^{(1)} &= 0\\
w^{(1)T} w^{(1)} + w^{(2)T} w^{(2)} - 1 &= 0\\
w^{(1)T} w^{(2)} &= 0\\
J_0^T v^{(1)} + \sum_{k=1}^{m} \left(J_k^T v^{(1)} c_k + J_k^T v^{(2)} s_k \right) - \omega v^{(2)} &\\
+\gamma_1 w^{(1)} - \gamma_2 w^{(2)} &= 0\\
J_0^T v^{(2)} + \sum_{k=1}^{m} \left(J_k^T v^{(2)} c_k + J_k^T v^{(1)} s_k \right) + \omega v^{(1)} &\\
+\gamma_1 w^{(2)} + \gamma_2 w^{(1)} &= 0\\
v^{(1)T} w^{(1)} + v^{(2)T} w^{(2)} - 1 &= 0\\
\sum_{k=1}^{m} \Big(v^{(1)T} J_k w^{(2)} \tau_k c_k - v^{(1)T} J_k w^{(1)} \tau_k s_k &\\
-v^{(2)T} J_k w^{(1)} \tau_k c_k - v^{(2)T} J_k w^{(2)} \tau_k s_k \Big) &\\
+v^{(1)T} w^{(2)} - v^{(2)T} w^{(1)} &= 0\\
\sum_{k=1}^{m} \Big(v^{(1)T} J_{k0} w^{(1)} c_k + v^{(1)T} J_{k0} w^{(2)} s_k &\\
+v^{(2)T} J_{k0} w^{(2)} c_k - v^{(2)T} J_{k0} w^{(1)} s_k \Big) &\\
+J_0^T u + v^{(1)T} J_{00} w^{(1)} + v^{(2)T} J_{00} w^{(2)} &= 0\\
r - \sum_{k=1}^{m} \Big(v^{(1)T} J_{k\alpha} w^{(1)} c_k + v^{(1)T} J_{k\alpha} w^{(2)} s_k &\\
+v^{(2)T} J_{k\alpha} w^{(2)} c_k - v^{(2)T} J_{k\alpha} w^{(1)} s_k \Big) &\\
-J_\alpha^T u - v^{(1)T} J_{0\alpha} w^{(1)} - v^{(2)T} J_{0\alpha} w^{(2)} &= 0,
\end{aligned}
$$

where $c_k := \cos(\omega\tau_k)$ and $s_k := \sin(\omega\tau_k)$ are introduced for brevity. The vector of auxiliary variables $\bar{x}^{(\mathrm{Hopf})}$ collects $w^{(1)} \in \mathbb{R}^{n_x}$, $w^{(2)} \in \mathbb{R}^{n_x}$, $v^{(1)} \in \mathbb{R}^{n_x}$, $v^{(2)} \in \mathbb{R}^{n_x}$, $u \in \mathbb{R}^{n_x}$, $\omega \in \mathbb{R}$, $\gamma_1 \in \mathbb{R}$, and $\gamma_2 \in \mathbb{R}$. The function $f : \mathbb{R}^{(m+1)n_x} \times \mathbb{R}^{n_\alpha} \mapsto \mathbb{R}^{n_x}$ defines the DDE (3). $J_0 \in \mathbb{R}^{n_x \times n_x}$ and $J_k \in \mathbb{R}^{n_x \times n_x}$, $k = 1, \ldots, m$, are the Jacobian matrices $\partial f/\partial x(t)$ and $\partial f/\partial x(t-\tau_k)$, respectively. $J_{00} \in \mathbb{R}^{n_x \times n_x \times n_x}$ and $J_{k0} \in \mathbb{R}^{n_x \times n_x \times n_x}$ denote second order derivatives $\partial f/(\partial x(t)\partial x(t))$ and $\partial f/(\partial x(t-\tau_k)\partial x(t))$. $J_{0\alpha} \in \mathbb{R}^{n_x \times n_x \times n_\alpha}$ and $J_{k\alpha} \in \mathbb{R}^{n_x \times n_x \times n_\alpha}$ refer to $\partial f/(\partial x(t)\partial\alpha)$ and $\partial f/(\partial x(t-\tau_k)\partial\alpha)$. A superscript T denotes vector or matrix transposition.